

Article

# Land Use Evaluation over the Jema Watershed, in the Upper Blue Nile River Basin, Northwestern Highlands of Ethiopia

Mintesinot Taye <sup>1,\*</sup> , Belay Simane <sup>2</sup>, Benjamin F. Zaitchik <sup>3</sup>, Yihenew G. Selassie <sup>4</sup> and Shimelis Setegn <sup>5</sup>

<sup>1</sup> Institute of Disaster Risk Management and Food Security Studies, Bahir Dar University, Bahir Dar 5501, Ethiopia

<sup>2</sup> Centre for Environment and Development Studies, Addis Ababa University, Addis Ababa 1176, Ethiopia; simaneb@yahoo.com

<sup>3</sup> Department of Earth and Planetary Sciences, Johns Hopkins University, Baltimore, MD 21218, USA; zaitchik@jhu.edu

<sup>4</sup> College of Agriculture and Environmental Sciences, Bahir Dar University, Bahir Dar 5501, Ethiopia; yihenewgs@gmail.com

<sup>5</sup> Environmental and Occupational Health, Florida International University, 11200 S.W. 8th st., Miami, FL 33199, USA; ssetegn@fiu.edu

\* Correspondence: mintesinotazene@yahoo.com; Tel.: +251-920-519737

Received: 7 February 2019; Accepted: 15 March 2019; Published: 19 March 2019



**Abstract:** Generating land capability class guidelines at a watershed scale has become a priority in sustainable agricultural land use. This study analyzed the area of cultivated land use situated on the non-arable land-capability class in the Jema watershed in the Upper Blue Nile River Basin. Soil surveys, meteorological ground observations, a digital elevation model (DEM) at 30 m, Meteosat at 10 km × 10 km and Landsat at 30 m were used to generate the sample soil texture class, average annual total rainfall (ATRF in mm), terrain, slope (%), elevation (m a.s.l) and land-use land cover (%). The land capability class was analyzed by considering raster layers of terrain, the average ATRF and soil texture. Geo-statistics was employed to fit a surface of soil texture and average ATRF estimates. An overlay technique was used to compute the proportion of cultivated land placed on non-arable land. As per the results of the terrain analysis, the elevation (m a.s.l) of the watershed is in the range of 1895 to 3518 m. The slope was found to be in the range of 0 to 45%. The amount of estimated rainfall ranged from 1640 to 131 mm with value declined from the lower to the higher elevation. Clay loam, clay and heavy clay were found to be the major soil texture classes. Four land capability classes, i.e., II, III, IV (arable) and V (non-arable), were identified with proportions of 28.56%, 45.74%, 22.16% and 3.54%, respectively. Seven land-use land covers were identified, i.e., annual crop land, grazing land, bush land, bare land, settlement land, forestland and water bodies, with proportions of 42.1, 35.9, 8.90, 8.3, 2.6, 2.1, and 0.2, respectively. Around 1707.7 ha of land in the watershed is categorized under non-arable land that cannot be used for annual crop cultivation at any level of intensity. Around 437 ha (3.5%) of land was cultivated on non-arable land. To conclude, the observed unsustainable crop land use could maximize soil loss in upstream regions and siltation and flooding downstream. The annual crop land use that was observed on non-arable land needs to be replaced with perennial crops, pasture and/or forest land uses.

**Keywords:** land use; sustainability; watershed; agroclimatic zones

## 1. Introduction

Agricultural production contributes to about 43% of the GDP, 80% of employment, and 75% of export in Ethiopia [1]. Meanwhile, ~80% of the population in the country lives in the highlands [2]. The study site, the Jema watershed, is situated in the north-western highland region of the country. This region is characterized by a complex topography and diverse agro-ecosystems [3]. A dramatic spatial heterogeneity was observed in terms of the steepness of slopes [4], soil features [5], and the climatic situation [6] in the region. The farming system relies on fragmented and small land holdings, i.e., 1.77 ha per household and mixed food crop and animal production at the subsistence scale [7]. Different land uses behave differently with respect to runoff and soil loss [8]. Protecting forest land contributes to the availability of more soil water in times of drought [9]. At a policy level, Ethiopia has planned to achieve a green economy through adopting a sustainable land management program [10]. In this regard, land capability class (LCC) guidelines at a watershed scale are crucial to indicate the general degree of limitation of land in terms of agricultural practice [11]. Slopes are believed to have a major role in determining the type of land use, mainly associated with its effect in runoff [12,13].

The amount of precipitation, soil type, land use and topography are the among the leading factors that control runoff in a watershed [9,14,15]. In this respect, the Ethiopian land-use policy discourages using land with slopes of 30% and above to cultivate annual crops [16]. Misuse of land including conversion of land use/cover is among the factors contributing to changes in watershed hydrology and the farming system. Land use change can affect runoff [15], flood frequency [17], base flow [18]. Forest land use/cover management can increase the total stream flow and groundwater recharge, leading to greater water supply during drought periods particularly within the context of a changing climate [19]. Accordingly, developing LCC guidelines is an essential component to explore the comparative advantages of various land segments and maximize their productivity [12,20]. In Ethiopia, the type of farming system, land use, amount of rainfall and soil type is determined by elevation [3,21–24]. Yet, land characterization studies [5,6,14,25,26] were made without considering agroclimatic zones.

LCC considers relatively permanent features of geographical sites, including elevation, slope, soil texture, stoniness, water logging, soil depth and rainfall [14,27]. To date, LCC guidelines that have been used across the world are primarily derived from the USDA's LCC [28]. In the USDA LCC system, land mapping units were classified into eight classes. The first four classes apply to arable land, in which the limitations on the use and need for conservation measures and careful management increase with class number; that is, the intensity of cultivation among arable LCCs varies from very intensive (LCC I) to limited (LCC IV). The remaining four classes are not suitable for cultivation, but can be used for pasture, woodland, wildlife, recreation and other purposes.

In previous empirical studies [25,29–32] conducted in the Upper Blue Nile River Basin where the study site is situated, seven major land use land cover (LULC) types were identified. These are crop land (cultivated and fallow land), bare land (rock outcrops and denuded land), bush land (scrub land), forested land (natural forests and plantations), woodland, grazing land (land under permanent pasture), settlement (scattered and nucleated rural villages), and water bodies (ponds, streams and springs).

However, land use has generally not fallen in line with the scientific LCC guidelines in Ethiopia [10]. For instance, cultivation for annual crop production was practiced on lands which need to be reserved for other purposes including animal husbandry, forestry and other non-cultivation activities. The existence of the problem has also been proved by studies conducted in the north-western highlands of the country [12,20,32]. These studies showed as subsistence crop production has expanded into ecologically marginal areas. This kind of unscientific conversion can adversely affect the erodibility of soil and observed erosion rates [33], hydrology [34], biodiversity [35], ecosystem services [36] and climate through its influence on the surface energy budget [37]. Consequently, soil erosion, siltation and water scarcity emerged as major problems for agriculture in the region [12,26]. The findings of these environmental studies emphasized the need to conduct LCC evaluation to inform land-use policy.

Nevertheless, to date, no such evaluation exists for the study watershed. The proportion of cultivated land that was utilized in contradiction to LCC guidelines has not been examined and documented. To address this need, the current study attempts an estimation of the proportion of the Jema watershed that is currently used for annual crop cultivation in a manner inconsistent with LCC guidelines. This study shows the methods and procedures of how to capture limitation of farmland taking into account more appropriate geographical unit of analysis, agroclimatic zones of a watershed. The same method could be implemented in tropical highlands where an ecosystem is complex like that of the study site.

## 2. Materials and Methods

### 2.1. Description of the Study Site

The Jema watershed is located within the area  $11^{\circ}22'0''$  N to  $11^{\circ}3'30''$  N and  $37^{\circ}2'0''$  E to  $37^{\circ}23'30''$  E (digital elevation model (DEM) at 30 m, shuttle radar topographic mission (SRTM)). The watershed belongs to part of the north-western highlands of Ethiopia in the Lake Tana Sub-Basin in the Upper Blue Nile River Basin (Figure 1). Its geographical area covers  $\sim 483$  km<sup>2</sup>. The area is situated in the West (*Mirab*) *Gojjam* Administrative Zone of the Amhara National Regional State. The topography of the site is characterized by gentle slopes, hilly landscape, and steep slopes, and the geology is dominated by volcanic rocks [38] of Late-Tertiary to Quaternary age. The site is categorized under semi-arid highland [10,24]. On average, its ATRF is  $\sim 1400$  mm, whereas its MT<sub>max</sub> and MT<sub>min</sub> are  $\sim 25$  °C and  $\sim 7$  °C, respectively. About 80% of the total precipitation occurs during the summer (*Kiremt*) season in the months of June, July and August. The maximum temperature has been recorded in March, during the spring (*Belg*) season in the months of March, April and May [39]. The main soil orders are Alisols, Nitisols and Vertisols [40]. The population density was estimated to be  $\sim 189.4$  persons/km<sup>2</sup> [41]. The primary livelihood is subsistence-scale mixed farming, i.e., food crop production and livestock rearing [7].

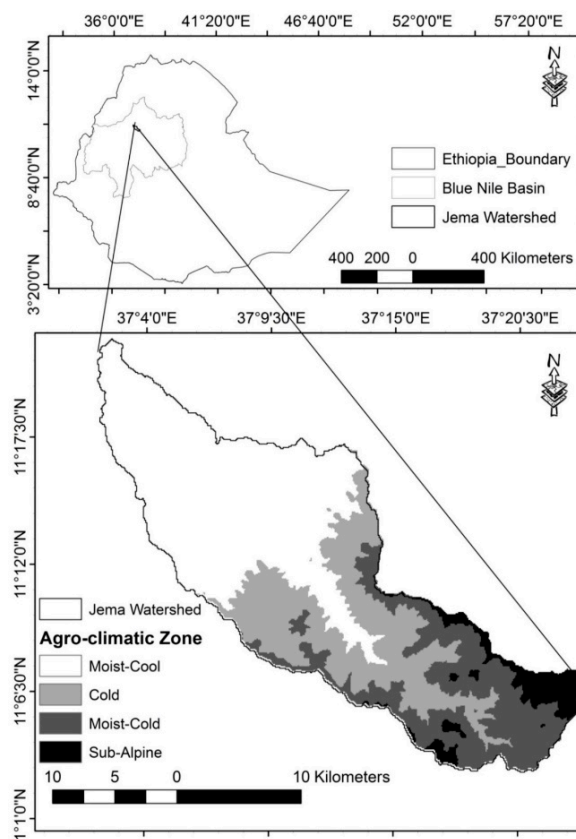


Figure 1. Location map of the Jema watershed and its agro-ecological zones.

## 2.2. Analysis of Land Capability Class (LCC)

LCC was examined considering soil texture (% of soil particle size), slope (%) and elevation (m), and the range of ATRF (mm). As stated in the work on the USDA system suggested by [42], in LCC analysis, the critical point is considering the degree of limitation of certain environmental variables; that is, a given LCC analysis is not required to consider the limitation of all environmental variables. The proportion of cultivated land use was also examined. Ultimately, the proportion of cultivated land situated on non-arable classes was computed.

### 2.2.1. Spatial Variability of ATRF

The rainfall data of this study were extracted from the estimated (reconstructed) data sets generated by Meteosat. The data were gridded at a spatial scale of 10 km × 10 km, and made for the years from 1983 to 2010. The reconstruction was done with the reference of observed data from 550 meteorological stations situated over Ethiopia. The data were reconstructed by the National Meteorological Agency of Ethiopia in collaboration with the International Research Institute for Climate and Society, USA. The data calibration and validation of this reconstructed data set was undertaken by Reading University, United Kingdom. The result showed a strong correlation (i.e.,  $r = 0.8$ ) between the station and satellite-derived data (Ethiopian Meteorological Agency cited in [6]). From the gridded Meteosat dataset, the value of 36 grid cells located inside and around the study watershed was considered. The sample values of the average ATRF were interpolated to the entire watershed, employing the most appropriate geospatial interpolation models.

The geospatial interpolation models were evaluated by comparing their relative committed root mean square error (RMSE) as in Equation (1). The analysis was done at the 95% confidence interval using ArcMap software. A model that might be found with the lowest value of RMSE was assumed to be the most optimal/accurate model to interpolate/estimate soil texture particles. The error value was expected to be in the range of the observed minimum and maximum values of an observed environmental attribute. The estimated value of a given environmental attribute with a model with the lowest RMSE value was expected to be closer to the measured values. In this estimation, the annual total rainfall (mm) data set was a predictand variable, and the elevation (meter) data set generated from the DEM 30 m was an auxiliary variable. Ordinary kriging (OK), simple kriging (SK), universal kriging (UK), disjunctive kriging (DK), simple cokriging (SCK), ordinary cokriging (OCK), universal cokriging (UK), inverse distance weighting (IDW), global polynomial interpolation (GPI), local polynomial interpolation (LPI), and radial basis function (RBF) were the interpolation models examined in the study. The first five models are stochastic, whereas the last four models are deterministic [43]. Unlike deterministic methods, stochastic (kriging and cokriging) interpolation methods can take into account the values of available relevant auxiliary variables to estimate the values of a given predictand variable. Since Ethiopian rainfall depends on topography, this study considered elevation as a co-variable. The application of these geo-statistical methods was recommended in previous studies [26,44,45].

$$\text{RMSE} = \left[ \frac{1}{n} \sum_{i=1}^n (p_i - o_i)^2 \right]^{1/2} \quad (1)$$

where RMSE is the root mean square error;  $n$  = number observations or samples;  $o$  = observed value at place  $i$ ;  $p$  = predicted/estimated value at place  $i$ ;  $osi$  = standardized observed value at place  $i$ ; and  $psi$  = standardized predicted/estimated value at place  $i$ .

### 2.2.2. Spatial Variability of Soil Texture

Soil sample sites and points were selected based on a two-stage cluster sampling technique accompanied by a stratified and proportionate sampling procedure. The sample strata were prepared considering the elevation and slope class variation of farmlands in the Jema watershed. Four elevation and seven slope sample strata were identified, and the numbers of soil and elevation classes was

decided following the recommendation of [24,27]. The strata of slopes were decided mainly based on the severity of soil erosion, whereas elevation strata were based on agro-climatic factors including the length of growing period. Both the watershed boundary and the terrain class maps (raster layers) were delineated from a satellite-derived 30 m resolution SRTM DEM (Figure 2). The accuracy of the map (DEM data) was verified by a ground truth field survey data collected by using a hand GPS (geographic positioning system) with a reported accuracy of 3–5 m. Once elevation and slope classes (the sample units or clusters) were identified, the specific farmland sample sites and points in each sample unit (that were assumed to be homogenous in terms of their biophysical setup) of soil were chosen depending on their accessibility.

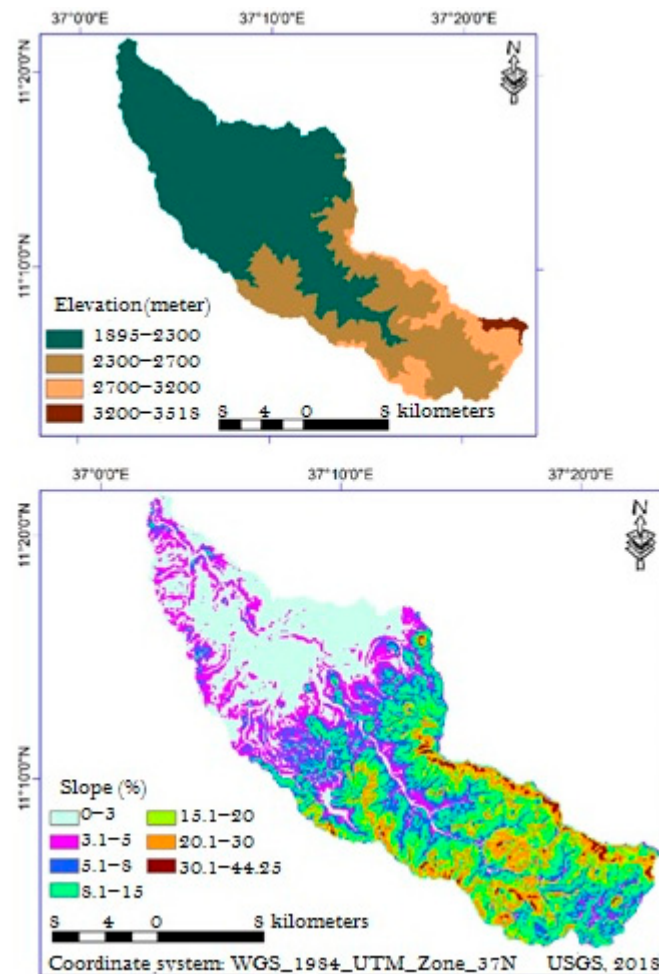


**Figure 2.** Elevation (m) and slope (%) classes of the Jema watershed.

A hand auger was used to collect sample soils. For testing soil texture, 36 composite (and disturbed) samples were collected from 36 farmland sites (sample units) situated in the stratified slope and elevation classes (Figure 2). Each farmland site covers an area of  $\sim 12.7 \text{ km}^2$ ; that is, the average spatial area coverage of each sample unit (farmland site) where one composite sample was collected. The scale of the map is categorized under a large-scale map (i.e., 1 cm to 2 km). One composite (and disturbed) soil sample was collected from 3 to 4 discrete sample points in the same sample site. In some steep slope sites, it was difficult to get the top soil. Thus, to homogenize the soil horizon where samples need to be taken, the samples for texture analysis were collected at a depth of 0–60 cm. The samples were analyzed in a soil laboratory following the procedure of ISRIC [46]. The texture samples were then dried in an oven and sieved through a 2 mm sieve.

In order to estimate the surface soil texture (sand, clay and silt particles) across the entire Jema watershed, the sample was subjected to geostatistical analysis. The same statistical tool, technique and procedure that were employed in the case of the rainfall interpolation were employed. Since temperature and gradient affect the nature of soil texture, both elevation and slope were considered as covariables. Finally, the raster surfaces of sand, clay and silt soil particles were combined and mapped into appropriate soil texture classes to the entire watershed. The texture class was determined by referring to the USDA's soil texture triangle.

### 2.2.3. Producing LCC Layer

Taking into account the observed degree of limitation in terrain (slope and elevation), average ATRF, and soil texture features, the LCC was determined. The degree of limitation and appropriate LCC were assigned by adapting the USDA's LCC guideline [27,42]. In the analysis of LCC, equal weight was given for all the aggregated values of categories/profiles (slope, soil texture, mean annual total rainfall and elevation). However, a different weight was attached to the diverse indicators identified under each category (Table 1).

**Table 1.** Land capability classes (LCCs) and their degree of limitation.

Categories/Profiles for Slope (%), Soil Texture (%), Mean Annual Total Rainfall (mm) and Elevation (m a.s.l)	LCCs and Their Degree of Limitation					
	I (0)	II (0.2)	III (0.4)	IV (0.6)	V (0.8)	VI (1)
Flat or almost flat (0–3)	x					
Gently sloping (3–8)		x				
Sloping (8–10%)		x				
Moderately steep (10–15)			x			
Steep (15–30)				x		
Very steep (30–44.25)					x	
Heavy clay				x		
Clay				x		
Clay loam		x				
Wet (>1400 mm)	x					
Moist (900–1400 mm)		x				
Moist–cool (1895–2300)	x					
Cold (2300–2700)		x				
Moist–cold (2700–3200)			x			
Sub-Alpine (3200–3518)				x		

Adapted from [27,42].

With respect to soil texture, a loam texture is associated with minimum limitation, and limitations increase as the texture diverges from loam in either direction [16]. Loam soil is believed to be the most optimal for plant growth with respect to air, water, mineral and nutrient circulation, which is vital for plant–soil interaction.

In general, as the slope of farmland increases, the limitation of land increases [16]. In the study region, the limitation of land also increases with elevation, as one moves from moist–cool to Alpine [24]. This is reflected in the terms “cultivable crop diversity” and “length of growing period” (LGP) [3, 47]. Based on the preliminary focus group discussion conducted in the ACZs of Jema watershed, crop diversity was found to be lower in the upstream region. With regard to LGP, there is a positive spatial association with elevation. The annual average ATRF was considered as an environmental factor in the LCC analysis because the study site is located in a semi-arid tropical region which requires more rainfall amount to maximize moisture availability and enhance land productivity. Moreover, together with the incoming solar radiation to be received at different elevation zones, differences in the average ATRF that is received in the cropping season may create variation in terms of crop type and diversity to be adapted, and water harvesting potential [24].

In order to produce one comprehensive LCC layer for the watershed, it was first essential to generate the same type of layers for soil, slope and elevation and average ATRF features separately. Then, the raster layers of the three variables were combined using a balanced weight overlay technique.

The degree of influence of the environmental variables in LCC analysis might not be the same. To date, there is no scientific guideline that shows the weights of indicators in terms of agricultural LCC analysis in the context of tropical highlands.

### 2.3. Spatial Variability of Land-Use Land Cover

The spatial variability of land-use land cover (LULC) was analyzed from Landsat8 scanned in January 2018, which is the dry season in the study region. The imagery was acquired from the United States Geological Survey (USGS) online data archive. The basic features of the imagery are given in Table 2.

**Table 2.** Characteristics of the satellite imagery used for analyzing land-use land cover classes.

Path and Raw Number of the Scene:	Path: 170, and Raw: 52
Number of bands (spectral resolution)	Out of 9 multispectral and 1 panchromatic band, red–green–blue (RGB), i.e., 4, 3 & 2 band combinations was used
Ground pixel size (spatial resolution)	Thirty meter resolution multispectral bands
Sensor name	Landsat 8
Product name	L1T
Cloud cover (%)	0.05
Reflectance bias	−0.100000

A total of 380 sample polygons were collected with the help of GPS for seven land-use land cover classes (grazing land, cultivated land/crop land, bush land, bare land, settlement land, forestland and water body) in the four ACZs of the watershed. For sampling purposes, the proportion of LULC types was estimated by visual observation made with the help of a field survey and Google Earth imagery. Nearly two-thirds of the total sample were used for training purposes, and the rest were reserved for validation. The imagery was analyzed employing the maximum likelihood classifier in a supervised classification method. It is recommended to employ this method especially in cases where the researcher has prior experience about the physical features of the site and could access the place for ground truthing [48,49]. Under supervised classification, the maximum likelihood classifier tool has been the most recognized tool of image classification.

The accuracy of the LULC classification analysis of this study was evaluated by calculating a confusion matrix (error matrix), including overall accuracy, producer's accuracy, and user's accuracy. Taking the statistical output of the confusion matrix, the Kappa statistic was computed. [50] suggested a kappa value of <40% as poor, 40% to 55% fair, 55% to 70% good, 70% to 85% very good and > 85% as excellent.

Ultimately, the non-arable land (i.e., LCC-V) raster layer and cultivated land raster layer were overlaid to identify any part of cultivated land situated on non-arable land. All statistics were computed using map algebra in ArcMap.

## 3. Results and Discussion

### 3.1. Spatial Pattern of Land Capability Class

#### 3.1.1. Surfacing the Spatial Distribution of the ATRF

Among all tested interpolation models, the OCK model provided the lowest RMSE when interpolating the average ATRF (RMSE = 0.72 mm). In this regard, the model was found to be the most optimal/accurate one, i.e., the estimated value with this model was close to the measured value. In the entire sample site, the estimated amount of the average ATRF increases as we go from north-west to south-east (Figure 3); that is, from the lower elevation to the higher elevation (Table 3).

Similarly, in the case of the specified study watershed, the amount of the average ATRF declines in the same direction. The value of the rainfall ranges from 1310 mm to 1640 mm in the study watershed. The figure shows the existence of a number of ups and downs in the values of the spatial distribution of the average ATRF in the whole sample site.

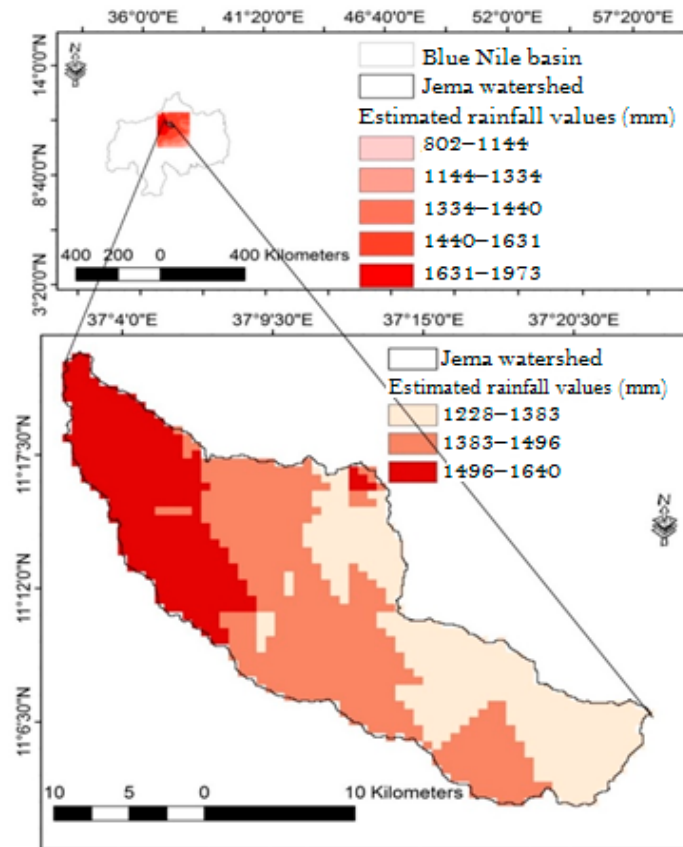


**Figure 3.** Kriged value of the average annual total rainfall (ATRF) by ordinary cokriging (OCK) for the entire interpolated surface.

**Table 3.** The kriged average values of the average annual total rainfall (ATRF) and temperature in the agroclimatic zones (ACZs) of the Jema watershed.

AEZ	Elevation (m)	ATRF (mm)	MTmax (°C)	MTmin (°C)
Moist–Cool	1895–2300	1497–1640	26.5	10.3
Cold	2301–2700	1381–1496	25.3	9.9
Moist–Cold	2701–3200	1311–1380	23.1	7.5
Sub-Alpine	3201–3518	1228–1310	21.0	4.7

Similar to the case study of [51] and in contrast to the national observation of [10], the result of this study showed that the amount of the ATRF declines from north-west to south-east. This happened in a situation where elevation increases as one moves from north-west to south-east. Nevertheless, the same pattern of mean ATRF was not observed across the study corners that were included in the interpolated surface. The reason for the observed patterns of rainfall could be an interactive effect of the direction of moist wind movement and microclimate factors.

Thus, in a river basin, where there is a complex topography and wind convection system, accurate and precise mean ATRF estimation needs micro-scale analysis.

The total moisture obtained from the rainwater, predominantly in the summer season, can be considered adequate to grow a wide range of local annual crops including barley (*Hordeum Vulgare*), wheat (*Triticum Spp.*), teff (*Eragrostis*), maize (*Zea Mays*), finger millet (*Eleusine Coracana*), sorghum

(*Sorghum Bicolor*), horse bean (*Vicia Faba*), pea (*Pisum Sativum*), lentil (*Lens Esculenta*), and potatoes (*Solanum Tuberosum*) [10]. However, apart from terrain and soil properties, the difference in the amount of temperature was important in determining the type of crop grown in the ACZs, as temperatures are cooler and the LGP is shorter at higher elevations.

### 3.1.2. Geo-Statistical Interpolation of Soil Texture

SCK (simple cokriging) of soil texture outperformed other kriging methods and deterministic interpolation models, as assessed by RMSE. SCK provided an accuracy of 86.5% for sand, 85.5% for clay, and 77% for silt. Heavy clay, clay, and clay loam were found as the major texture classes in the lower, middle and higher elevations, respectively (Table 4 and Figure 4). This indicates the complexity of the terrain in the study site. The result implies the existence of a spatial autocorrelation between soil texture and terrain attributes. Thus, the result was consistent with the theory of catenary soil development [52]. In the catenary soil development approach, there is a sequence of soils down a slope, created by the balance of processes such as precipitation, infiltration, and runoff. Catenary soil development is mainly true for relatively permanent soil properties such as texture [53].

**Table 4.** Area coverage of soil texture classes for the Jema watershed.

Texture Class	Area Coverage (km <sup>2</sup> )	Area Coverage (%)
Heavy clay	184.940	38.217
Clay	254.402	52.572
Clay loam	44.571	9.211
Total	483.915	100

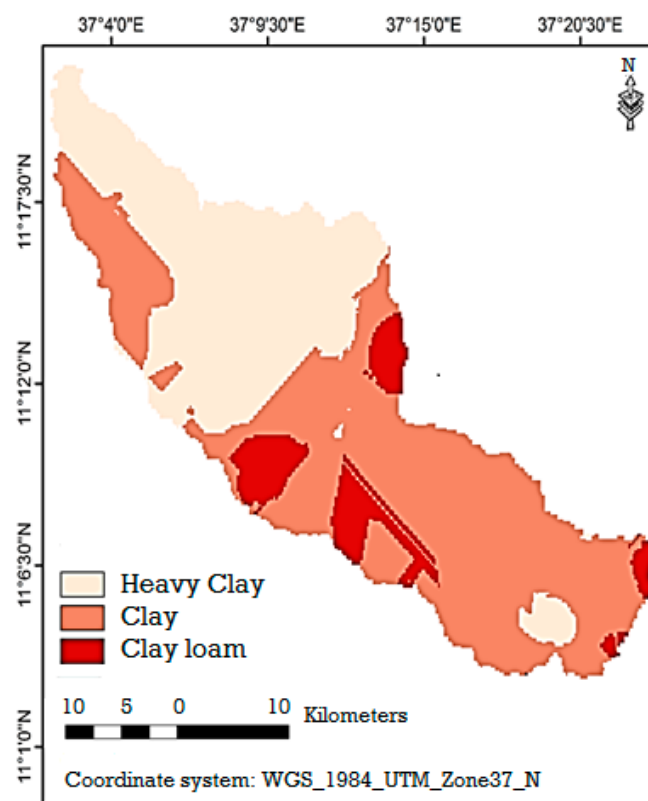


**Figure 4.** Predicted output surface for the combined soil particles (texture class).

The findings of this study contrast with the results of [5] that was conducted at the national level. In that study, the texture class of the Jema watershed was condensed only to the clay texture

class. Similarly, as inconsistent with the result of [5,24], the ATRF of the study watershed declines with elevation. The different findings might be attributed to the differences in the geographical scale of analysis and the complexity of the terrain in the north-western part of the country. Looking at the nature of soil texture, the water holding capacity of the soil can be regarded as low in the entire watershed and is especially limited in the downstream portion of the watershed. This signified the prevalence of erosion upstream and siltation downstream.

### 3.1.3. Land Capability Class

Based on the result of LCC analysis that was conducted, considering slope (%), elevation (m), soil texture (%) and average ATRF (mm), four (II, III, IV and V) USDA LCC were identified (Figure 5). Their area coverage was calculated for the entire Jema watershed (Table 5) and for each AEZ of the watershed (Table 6). Most of the land in the watershed was characterized by LCC-III, while LCC-V was found only in the two ACZs (sub-Alpine and moist-cold) situated in the higher elevation.

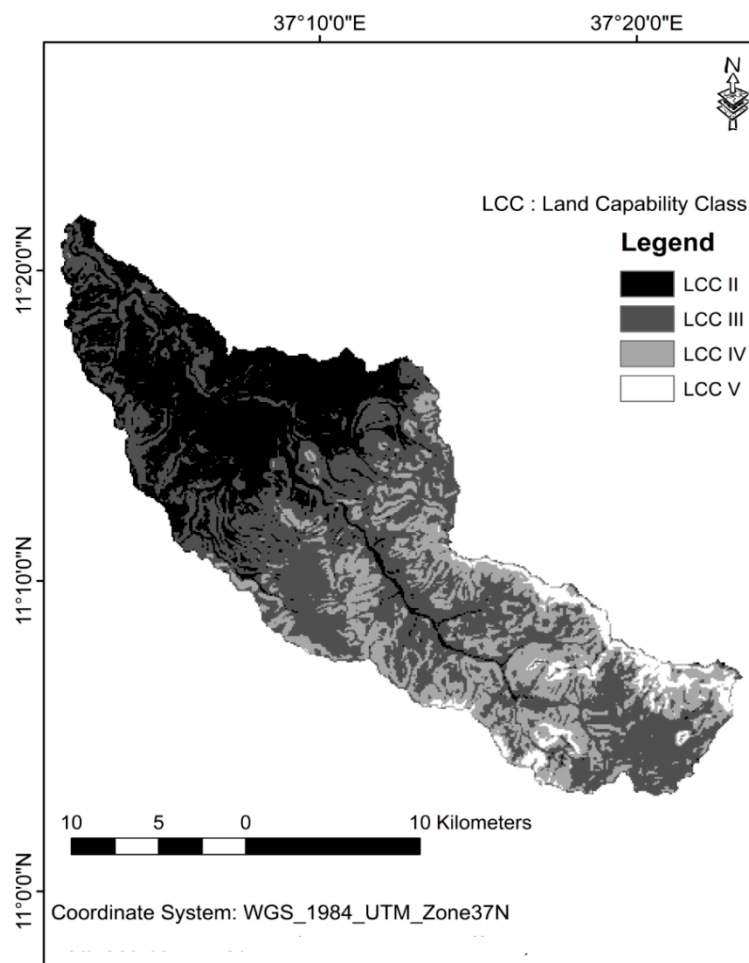


**Figure 5.** The distribution of LCC among the agro-ecological zones of the Jema watershed.

**Table 5.** Area coverage of different LCCs in the entire study site.

LCC	Area Coverage (ha)	Area Coverage (%)
II	13,778.71	28.56
III	22,067.29	45.74
IV	10,690.41	22.16
V	1707.72	3.54
Total	48,244.12	100

**Table 6.** Area coverage land capability classes (LCCs) among the ACZs of the study site.

LCC	Area Coverage (%) in Each of the ACZ			
	Moist–Cold (1895–2300 m a.s.l)	Cold (2301–2700 m a.s.l)	Moist–Cool (2701–3200 m a.s.l)	Sub-Alpine (3201–3518 m a.s.l)
II	47.92	0.00	0.56	1.75
III	43.75	59.07	16.00	12.82
IV	8.34	40.93	46.66	52.62
V	0.00	0.00	36.78	32.82

Most (~96.5%) of the land in the Jema watershed could be categorized as some category of arable land; the remaining portion was non-arable. Though very intensive cultivation cannot be exercised in the entire watershed, limited cultivation with proper land management can be exercised all over the watershed except on LCC-V (3.5%) of the watershed. Much of the land with LCC-V was situated in the higher elevation areas, sub-Alpine and moist–cold ACZs. In the study conducted in the Guila-Abena watershed in northern Ethiopia [54], four major LCCs (II, III, IV and V) were identified. In the study of [14] conducted in the Gido watershed in northern Ethiopia, the capability of the land fell into four classes ranging from I to IV.

### 3.2. Spatial Variability of Land-Use Land Cover

The overall statistical error report of the image classification is shown in Table 7. The highlighted frequency values represent the main diagonal of the matrix that contain the cases where the class labels depicted in the image classification and ground dataset matching, whereas the off-diagonal elements contain those cases where a mismatch in the labels was indicated.

**Table 7.** Error matrix (accuracy assessment report) made for the classified LULC analysis.

Predicted Class	True Class							Total	User's Accuracy (%)
	1	2	3	4	5	6	7		
1	17	0	3	0	0	2	0	22	77.27
2	0	14	0	1	1	0	0	16	87.50
3	2	0	23	0	0	0	1	26	88.46
4	0	1	0	19	0	0	0	20	95.00
5	1	0	0	0	12	0	0	13	92.31
6	0	0	0	0	0	11	2	13	84.62
7	0	0	0	1	0	3	10	14	71.43
Total	20	15	26	21	13	16	13		OAA = 85.48
Producer's Accuracy (%)	85.00	93.33	88.46	90.48	92.31	68.75	76.92		(%)

OAA: overall accuracy; 1: bare land, 2: bush land, 3: cultivated land, 4: forested & plantation area, 5: grazing land, 6: residential land, 7: water bodies.

Thus, with regard to overall accuracy, 85.48% of the classification was found to be accurate. With respect to reliability (Kappa Coefficient), the classification was 82.4% better than would have occurred strictly by chance. The result revealed that the proportion of grazing land, crop land (cultivated land), bush land, bare land, settlement land, forest land and water bodies were 42.09%, 35.90%, 8.95%, 8.27%, 2.58%, 2.05% and 0.17%, respectively (Figure 6 and Table 8). Most of the area was used for and/or covered with grazing land and crop land. It was found out that a larger proportion of cultivable land is situated downstream.

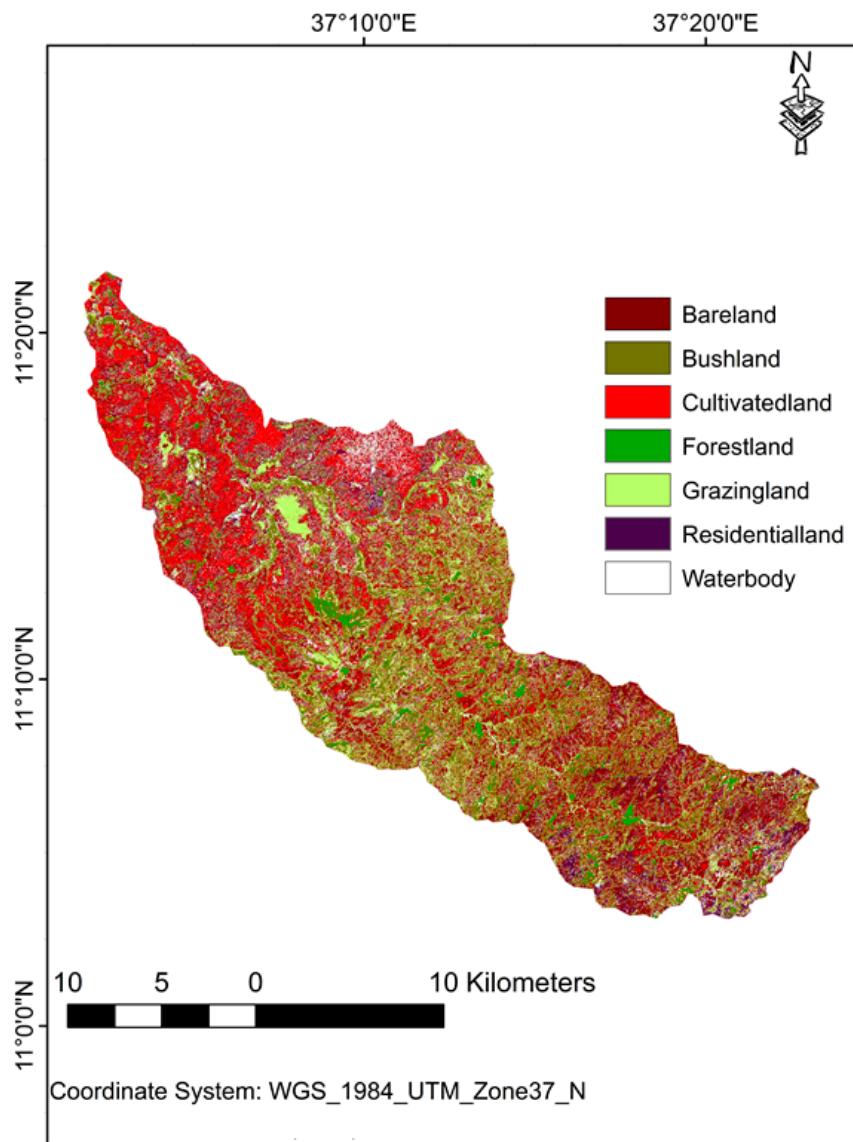


**Figure 6.** The spatial distribution of land-use land cover in the Jema watershed.

**Table 8.** Area coverage (and proportion) of the classified LULC types among the ACZs of the Jema watershed.

LULC Types	Area Coverage and Proportion in the ACZs							
	Moist–Cool Highland		Cold		Moist–Cold		Sub-Alpine	
	Area (ha)	%	Area (ha)	%	Area (ha)	%	Area (ha)	%
Bare land	1915.61	6.67	1357.99	9.14	687.38	16.00	38.03	8.28
Bush land	2307.80	8.04	1659.96	11.17	292.32	6.81	59.00	12.85
Cultivated land	12,230.10	42.61	3768.01	25.35	1266.35	29.48	91.22	19.87
Forested land	367.83	1.28	473.00	3.18	139.39	3.25	6.39	1.39
Grazing land	11,071.44	38.57	7270.90	48.93	1737.34	40.45	249.01	54.25
Settlement land	758.12	2.64	305.82	2.06	169.18	3.94	14.67	3.20
Water bodies	50.69	0.18	25.58	0.17	3.40	0.08	0.68	0.15
Total	28,701.59	100	14,861.25	100	4295.34	100	458.98	100

Given the proportion of bare land and bush land (Table 8), the agro-ecosystem of the entire watershed could be regarded as sensitive to climate variability. In addition, since most of the forest

cover was dominated by eucalyptus trees that have sparse canopies (local farmers-focus group discussion made in 2017), the existing limited forest would have little potential to reduce run-off [11]. Accordingly, cultivated lands are most likely to face severe soil loss, predominantly in parts of the watershed where the slope is steep. As shown by [31,55], such places would be subject to high surface runoff and low water retention.

### 3.3. Cultivated Land Use versus Arable Land Capability Class

Overlaying the LCC V layer extracted from the LCC layer (Figure 5) over the cultivated land use layer extracted from the land-use land cover layer (Figure 6), it was possible to find ~437 ha of cultivated land on potentially non-arable land in the upstream. This study proved that a good part of the land segments was not utilized in accordance with their comparative advantages, i.e., LCC guidelines. This may be due to the scarcity of farmland induced by the high annual total population growth rate (3% per year at regional level [2], the expansion of gullies in cultivated areas, the prevailing high soil loss rate (300+ tons/ha/year at the national level [24], and the low penetration of agricultural technologies. All of these pressures can lead farmers to encroach onto non-arable and steep slope land segments for cultivation and settlement purposes. General issues of low productivity and poverty [10] accompanied by weak land use and land administration institutions [1] can also contribute to this encroachment into marginal lands. Studies conducted in the Ethiopian highlands indicated that the way some farmers utilize and conserve their land and environment was not in line with the capability of the land [9,12]. If the same pattern of misuse of land continues, runoff [15], flood frequency [17], drought periods [9,19] could be intensified. As per the result of the current study, homogenizing a watershed into ACZs would enable researchers and policy makers to easily target specific sites where misuse of land is concentrated.

Accordingly, unless the ongoing poverty reduction program introduces safety nets to enhance non-cultivation and alternative livelihood strategies, 3.5% (437 ha) of the land that is being used for crop cultivation will become more exposed to soil loss. Since this endangered land is situated in the upstream portion of the watershed, its adverse impacts would extend to downstream areas in various forms. For example, it could aggravate the problem of siltation and minimize the volume of surface stream flow. As a result, the productivity of farming systems would be affected negatively.

## 4. Conclusions and Recommendations

Analysis of LCC taking into account the ACZs of a watershed was found to be more appropriate in terms of capturing the limitations of farming land. Accordingly, taking into account the limitations of land (soil texture, slope, elevation and mean ATRF), ~3.5% (1707.72 ha) of the watershed should not be used for cultivation at any level of intensity. The degree of land limitation is larger in the upstream portion of the watershed. At present, out of the total non-arable land, 437 ha was cultivated for crop production. To limit land degradation, farmers who settle on this non-arable land should change their way of using their land from annual crop production into perennial crops (fruit), pasture or forestry. These land uses can also be made to be more effective through the proper integration of forage legumes with agro-forestry systems, the expansion of perennial grasses, bunds, grass strips, contour leveling, terraces, shade trees and waterways. Through the expansion of farming practices such as the rotation of grazing and promotion of stall feeding, the practice of pasture land use and livestock rearing would be more effective. Meanwhile, the local government should be more committed to enforcing land use regulations through strengthening natural resource conservation bylaws.

**Author Contributions:** Conceptualization, M.A.T.; Formal analysis, M.A.T.; Investigation, M.A.T.; Methodology, M.A.T.; Supervision, B.S., B.F.Z., S.S. and Y.G.S.; Writing—original draft, M.A.T.

**Funding:** Belmont Forum, via NSF award ICER-1624335.

**Acknowledgments:** Florida International University, USA, is appreciated for hosting the senior author as a visiting scholar.

**Conflicts of Interest:** The authors declare no conflicts of interest.

## References

1. Ministry of Finance and Economic Development (MOFED). *Ethiopia's Climate-Resilient Green Economy, Green Economy Strategy*; Federal Democratic Republic of Ethiopia: Addis Ababa, Ethiopia, 2011.
2. Central Statistics Agency (CSA). *Summary and Statistical Report of the 2007 Population and Housing Census Results*; UNFPA: Addis Ababa, Ethiopia, 2008; p. 83.
3. Simane, B.; Zaitchik, B.F.; Foltz, J.D. Agroecosystem specific climate vulnerability analysis: Application of the livelihood vulnerability index to a tropical highland region. *Mitig. Adapt. Strateg. Glob. Chang.* **2014**, *21*, 39–65. [[CrossRef](#)] [[PubMed](#)]
4. Zaitchik, B.F.; Simane, B.; Habib, S.; Anderson, M.C.; Ozdogan, M.; Foltz, J.D. Building climate resilience in the Blue Nile/Abay Highlands: A role for earth system sciences. *Int. J. Environ. Res. Public Health* **2012**, *9*, 435–461. [[CrossRef](#)] [[PubMed](#)]
5. Berhanu, B.; Melesse, A.M.; Seleshi, Y. GIS-based hydrological zones and soil geo-data base of Ethiopia. *Catena* **2013**, *104*, 21–31. [[CrossRef](#)]
6. Mengistu, D.; Bewket, W.; Lal, R. Recent spatiotemporal temperature and rainfall variability and trends over the Upper Blue Nile River Basin, Ethiopia. *Int. J. Climatol.* **2014**, *34*, 2278–2292. [[CrossRef](#)]
7. Central Statistics Authority (CSA). *The World Bank. Ethiopia Rural Socioeconomic Survey (ERSS)*; CSA: Addis Ababa, Ethiopia, 2013.
8. Genet, A.; Sebat, M. Rainfall, Runoff and Soil loss, relationship on different land uses in the Upper Lake Tana Basin. *J. Agric. Environ. Int. Dev.* **2018**, *112*, 3–23.
9. Luo, P.; He, B.; Duan, W.; Takara, K.; Nover, D. Impact assessment of rainfall scenarios and land-use change on hydrologic response using synthetic Area IDF curves. *J. Flood Risk Manag.* **2018**, *11*, S84–S97. [[CrossRef](#)]
10. Ministry of Agriculture and Rural Development (MOARD). *Agroecological Zonation of Ethiopia*; MOARD: Addis Ababa, Ethiopia, 2000.
11. Food and Agriculture Organization (FAO). *Land Evaluation towards a Revised Framework*; Land and Water Discussion Paper; FAO: Rome, Italy, 2007; Volume 6.
12. Zeleke, G.; Hurni, H. Implications of land use and land cover dynamics for mountain resource degradation in the Northwestern Ethiopian Highlands. *Mount. Res. Dev.* **2001**, *21*, 184–191. [[CrossRef](#)]
13. Landon, J.R. *Booker Tropical Soil Manual: A Handbook for Soil Survey and Agricultural Land Evaluation in the Tropics and Subtropics*; Routledge: Abington, UK, 2014.
14. Tegene, B. Combining land capability evaluation, geographic information systems, and indigenous technologies for soil conservation in northern Ethiopia. *East. Afr. Soc. Sci. Res. Rev.* **2003**, *19*, 23–53. [[CrossRef](#)]
15. Luo, P.; He, B.; Takara, K.; Xiong, Y.E.; Nover, D.; Duan, W.; Fukushi, K. Historical assessment of Chinese and Japanese flood management policies and implications for managing future floods. *Environ. Sci. Policy* **2015**, *48*, 265–277. [[CrossRef](#)]
16. Anonymous. *Amhara National Regional State Environmental Protection, Land Administration and Use Authority (ANRSEPLAA)*; The Revised Rural Land Administration and Use Determination Proclamation, No. 133/200; FAO: Addis Ababa, Ethiopia, 2006; pp. 11–70.
17. Brath, A.; Montanari, A.; Moretti, G. Assessing the effect on flood frequency of land use change via hydrological simulation (with uncertainty). *J. Hydrol.* **2006**, *324*, 141–153. [[CrossRef](#)]
18. Wang, G.; Zhang, Y.; Liu, G.; Chen, L. Impact of land-use change on hydrological processes in the Maying River basin, China. *Sci. China Ser. D Earth Sci.* **2006**, *49*, 1098–1110. [[CrossRef](#)]
19. Van Dijk, A.I.; Beck, H.E.; Crosbie, R.S.; de Jeu, R.A.; Liu, Y.Y.; Podger, G.M.; Timbal, B.; Viney, N.R. The Millennium Drought in southeast Australia (2001–2009): Natural and human causes and implications for water resources, ecosystems, economy, and society. *Water Resources Research* **2013**, *49*, 1040–1057. [[CrossRef](#)]
20. Hurni, H.; Tato, K.; Zeleke, G. The implications of changes in population, land use, and land management for surface runoff in the upper Nile basin area of Ethiopia. *Mount. Res. Dev.* **2005**, *25*, 147–154. [[CrossRef](#)]
21. Taye, M.; Simane, B.; Selssie, Y.; Zaitchik, B.; Setegn, S. Analysis of the Spatial Variability of Soil Texture in a Tropical Highland: The Case of the Jema Watershed, Northwestern Highlands of Ethiopia. *Int. J. Environ. Res. Public Health* **2018**, *15*, 1903. [[CrossRef](#)]

22. Taye, M.; Simane, B.; Zaitchik, B.; Setegn, S.; Selassie, Y. Analysis of the Spatial Patterns of Rainfall across the Agro-Climatic Zones of Jema Watershed in the Northwestern Highlands of Ethiopia. *Geosciences* **2019**, *9*, 22. [[CrossRef](#)]
23. Tessema, I.; Simane, B. Vulnerability analysis of smallholder farmers to climate variability and change: An agro-ecological system-based approach in the Fincha'a sub-basin of the upper Blue Nile Basin of Ethiopia. *Ecol. Process.* **2019**, *8*, 5. [[CrossRef](#)]
24. Hurni, H. Degradation and conservation of the resources in the Ethiopian highlands. *Mount. Res. Dev.* **1988**, *8*, 123–130. [[CrossRef](#)]
25. Teferi, E.; Bewket, W.; Uhlenbrook, S.; Wenninger, J. Understanding recent land use and land cover dynamics in the source region of the Upper Blue Nile, Ethiopia: Spatially explicit statistical modeling of systematic transitions. *Agric. Ecosyst. Environ.* **2013**, *165*, 98–117. [[CrossRef](#)]
26. Setegn, S.G.; Srinivasan, R.; Dargahi, B.; Melesse, A.M. Spatial delineation of soil erosion vulnerability in the Lake Tana Basin, Ethiopia. *Hydrol. Process.* **2009**, *23*, 3738–3750. [[CrossRef](#)]
27. Davidson, D.A. *The Evaluation of Land Resources*; Longman Scientific: London, UK, 1992.
28. Klingebiel, A.A.; Montgomery, P.H. *Land-Capability Classification. Agricultural Handbook, No. 210*; Soil Conservation Service, US Department of Agriculture: Washington, DC, USA, 1961.
29. Minale, A.S.; Rao, K.K. Impacts of land cover/use dynamics of Gilgel Abbay catchment of Lake Tana on climate variability, Northwestern Ethiopia. *Appl. Geomat.* **2012**, *4*, 155–162. [[CrossRef](#)]
30. Amsalu, A.; de Graaff, J. Farmers' views of soil erosion problems and their conservation knowledge at Beressa watershed, central highlands of Ethiopia. *Agric. Hum. Values* **2006**, *23*, 99–108. [[CrossRef](#)]
31. Bewket, W. Towards Integrated Watershed Management in Highlands of Ethiopia: The Chemoga Watershed Case. Ph.D. Thesis, Wageningen University and Research Centre, Wageningen University Research, Wageningen, The Netherlands, 2003.
32. Bewket, W.; Teferi, E. Assessment of soil erosion hazard and prioritization for treatment at the watershed level: Case study in the Chemoga watershed, Blue Nile basin, Ethiopia. *Land Degrad. Dev.* **2009**, *20*, 609–622. [[CrossRef](#)]
33. Morgan, R.P.C. *Soil Erosion and Conservation*, 2nd ed.; Longman Group Unlimited: London, UK, 1995.
34. Uhlenbrook, S. Biofuel and water cycle dynamics: What are the related challenges for hydrological processes research? *Hydrol. Process.* **2007**, *21*, 3647–3650. [[CrossRef](#)]
35. Hansen, A.J.; DeFries, R.S.; Turner, W. *Land Use Change and Biodiversity: A Synthesis of Rates and Consequences during the Period of Satellite Imagery Land Change Science*; Gutman, G., Janetos, A.C., Justice, C.O., Moran, E.F., Mustard, J.F., Rindfuss, R.R., Skole, D.L., Turner, B.L., Cochrane, M.A., Eds.; Springer: Dordrecht, The Netherlands, 2004; pp. 277–299.
36. DeFries, R.; Bounoua, L. Consequences of land use change for ecosystem services: A future unlike the past. *GeoJournal* **2004**, *61*, 345–351. [[CrossRef](#)]
37. Pongratz, J.; Reick, C.H.; Raddatz, T.; Claussen, M. Effects of anthropogenic land cover change on the carbon cycle of the last millennium. *Glob. Biogeochem. Cycles* **2009**, *23*, 1–13. [[CrossRef](#)]
38. Poppe, L.; Frankl, A.; Poesen, J.; Admasu, T.; Dessie, M.; Adgo, E.; Deckers, J.; Nyssen, J. Geomorphology of the Lake Tana basin, Ethiopia. *J. Maps* **2013**, *9*, 431–437. [[CrossRef](#)]
39. National Meteorological Agency (NMA). *Initial National Communication of Ethiopia to the United Nations Framework Convention on Climate Change (UNFCCC)*; NMA: Addis Ababa, Ethiopia, 2007.
40. Food and Agricultural Organization (FAO); ISSS Illinois. *World Reference Base for Soil Resources*; World Soil Resources Reports 84; FAO: Rome, Italy, 1998.
41. Bureau of Finance and Economic Development (BOFED). *Population Affaires Core Process Based on 2012 Inter-Censal Survey*; Amhara National Regional State Development Indicator 2014/15; Amhara National Regional State: Bair Dar, Ethiopia, 2014.
42. Young, A. *Tropical Soils and Soil Survey*; Cambridge Geographical Studies 9; Paperback Edition; Cambridge University Press: Cambridge, UK, 1976.
43. Environmental Systems Research Institute (ESRI). *ArcGIS Desktop: Release 10.2.2*; Environmental Systems Research Institute: Redlands, CA, USA, 2014.
44. Mohammad, Z.M.; Taghizadeh-Mehrjardi, R.; Akbarzadeh, A. Evaluation of geostatistical techniques for mapping spatial distribution of soil pH, salinity and plant cover affected by environmental factors in Southern Iran. *Notulae Sci. Biol.* **2010**, *2*, 92–103.

45. Robinson, T.P.; Metternicht, G. Testing the performance of spatial interpolation techniques for mapping soil properties. *Comput. Electron. Agric.* **2006**, *50*, 97–108. [[CrossRef](#)]
46. International Soil Reference and Information Centre (ISRIC). *Procedures for Soil Analysis. Technical Paper*, 6th ed.; ISRIC: Wageningen, The Netherlands, 2002; ISBN 90-6672-044-1.
47. Asmare, B.; Mekuriaw, Y.; Tekliye, L. Evaluation of desho grass (*Pennisetum pedicellatum* Trin.) morphology, yield and chemical composition under irrigation in northwestern Ethiopia. *J. Agric. Environ. Int. Dev.* **2018**, *112*, 241–252.
48. Bartholomé, E.; Belward, A.S. GLC2000: A new approach to global land cover mapping from Earth observation data. *Int. J. Remote Sens.* **2005**, *26*, 1959–1977. [[CrossRef](#)]
49. Lillesand, T.; Kiefer, R.W.; Chipman, J. *Remote Sensing and Image Interpretation*; John Wiley & Sons: Hoboken, NJ, USA, 2014.
50. Monserud, R.A. *Methods for Comparing Global Vegetation Maps*; International Institute for Applied Systems Analysis: Laxenburg, Austria, 1990.
51. Conway, D. The climate and hydrology of the Upper Blue Nile River. *Geogr. J.* **2000**, *166*, 49–62. [[CrossRef](#)]
52. Webster, R. *Soil Science and Geostatistics. Soil Geography and Geostatistics-Concepts and Applications*; European Commission, Joint Research Centre, Institute for Environment and Sustainability: Copenhagen, Denmark, 2008; pp. 1–11.
53. Bockheim, J.G.; Gennadiyev, A.N.; Hammer, R.D.; Tandarich, J.P. Historical development of key concepts in pedology. *Geoderma* **2005**, *124*, 23–36. [[CrossRef](#)]
54. Ahmed, A.S.; Kebede, F.; Haile, M. Land Capability Classification and growing period for Guila Abena Watershed in Sassie Tseda Emba District in Eastern Tigray, Ethiopia. *Nat. Sci.* **2010**, *8*, 237–243.
55. Setegn, S.G.; Rayner, D.; Melesse, A.M.; Dargahi, B.; Srinivasan, R. Impact of climate change on the hydroclimatology of Lake Tana Basin, Ethiopia. *Water Resour. Res.* **2011**, *47*. [[CrossRef](#)]



© 2019 by the authors. Licensee MDPI, Basel, Switzerland. This article is an open access article distributed under the terms and conditions of the Creative Commons Attribution (CC BY) license (<http://creativecommons.org/licenses/by/4.0/>).